

Miniaturized Optical Particle Manipulation with Integrated VCSEL Arrays

Anna Bergmann

In recent years, optical manipulation has gained increasing interest, especially in combination with microfluidics. The contamination-free handling of micrometer-sized particles without any mechanical contact is an attractive tool for biology and medicine. VCSELs (vertical-cavity surface-emitting lasers) are an excellent choice for the trapping lasers, offering the opportunity of miniaturization by means of integration, and of parallel particle manipulation by using two-dimensional VCSEL arrays.

In this report, we present a novel concept for the realization of the so-called integrated optical trap. For this purpose, AlGaAs–GaAs-based VCSEL arrays with a very small device pitch were fabricated. We show the realization of integration-ready particle manipulation devices.

1. Introduction

The fact that the radiation pressure exerted by a laser beam is able to accelerate particles was first reported by Arthur Ashkin in 1970 [1]. This pressure is commonly called scattering force. Additionally, he discovered a second, unexpected force, pulling particles towards the center of the laser beam. This effect can be explained considering the momentum transfer from the incident laser beam to transparent particles, assuming a laser beam with a transverse intensity gradient, as shown in Fig. 1. The beam rays incident to the particle are refracted at the particle surface, resulting in a force oriented orthogonal to the beam propagation direction. For two exemplary rays A and B , with A closer to the beam center and thus having a higher intensity than B , the force F_A caused by ray A is larger than the force F_B , giving rise to a net force pulling the particle towards the intensity maximum, or towards the beam center. As this force is based on the transverse intensity gradient, it is commonly called transverse gradient force. It is exploited in so-called optical traps or optical tweezers, of which the latter was discovered in 1986 by Arthur Ashkin [2]. Here, a strong focusing of the laser beam is needed. The focusing provides an additional intensity gradient in longitudinal direction, pulling particles to the focal point (Fig. 2). If the longitudinal gradient force exceeds the scattering force, stable three-dimensional trapping can be achieved. Optical manipulation covers an important area of research dealing with the handling and trapping of nanometer- to micrometer-sized particles. It is a field of interest mainly for biology and medicine offering the big advantage of handling biological material without contamination or mechanical damage [3].

The field of microfluidics has rapidly expanded since the development of the first microfluidic devices in the early 1990s [4]. Microfluidic channels enable the examination

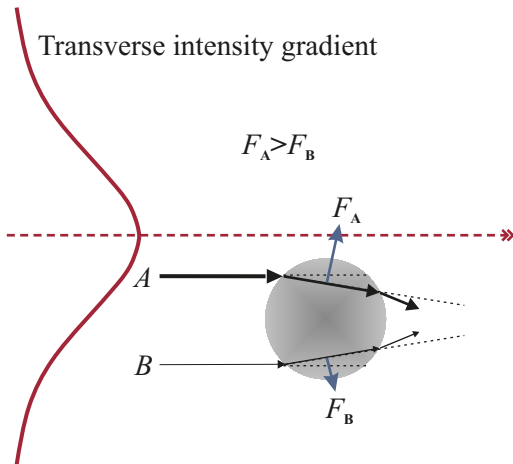


Fig. 1: Working principle of a two-dimensional optical trap. A laser beam with a transverse intensity gradient is refracted at the transparent, spherical particle, resulting in forces by momentum transfer. The net force points towards the intensity maximum.

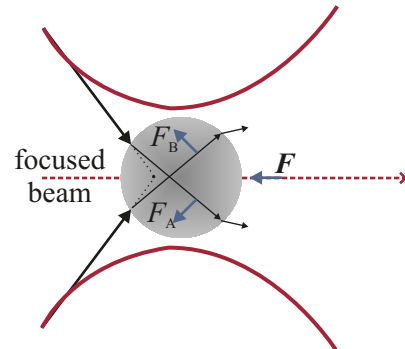


Fig. 2: Working principle of three-dimensional optical tweezers. Due to tight focusing, the laser beam has a longitudinal intensity gradient. If the longitudinal gradient force overcomes the scattering force, the particle is three-dimensionally trapped.

of biological samples with strongly reduced sample volumes, parallel cycling and exact timing [5, 6]. For the handling of particles inside the channels without additional tools like valves, electroosmotic or hydrodynamic setups, microfluidics and optical manipulation were successfully combined [7, 8]. With the driving force of miniaturization in almost all areas, the use of vertical-cavity surface-emitting lasers (VCSELs) as laser sources has gained increasing interest [8–13]. Their advantageous properties make them highly suitable for optical manipulation in microfluidics. One advantage of VCSELs is their emission in the near-infrared range. Since biological material has only little absorption at these wavelengths, the risk of thermal damage is minimized. Because of their vertical emission, which allows the comparatively easy fabrication of two-dimensional laser arrangements (arrays), patterns of multiple optical traps can be generated without the need for extensive beam splitting or steering setups. Besides the classical tweezers setup, even a drastically miniaturized setup can be envisioned. By directly integrating VCSEL arrays and microfluidic channels, a portable, low-cost particle manipulation device is feasible, whereas one can hardly imagine the realization of similar integrated modules with other laser sources.

2. VCSEL Arrays as Laser Sources for Optical Manipulation in Microfluidics

The schematic structure of a top-emitting VCSEL is depicted in the left part of Fig. 3. It is grown in the AlGaAs material system using molecular beam epitaxy, with a structure designed for an emission wavelength of around 850 nm. The laser resonator is built by distributed Bragg reflector (DBR) mirrors. Both the bottom DBR and the GaAs substrate

underneath are n-doped to enable back side contacting. The top DBR is p-doped and has a reduced number of mirror pairs compared to the n-type DBR. As this is the light outcoupling side of the VCSEL, the top p-contact is structured as a ring on top of the mesa. The active region in the inner cavity consists of three 8 nm thick GaAs quantum wells, separated by 10 nm thick barriers.

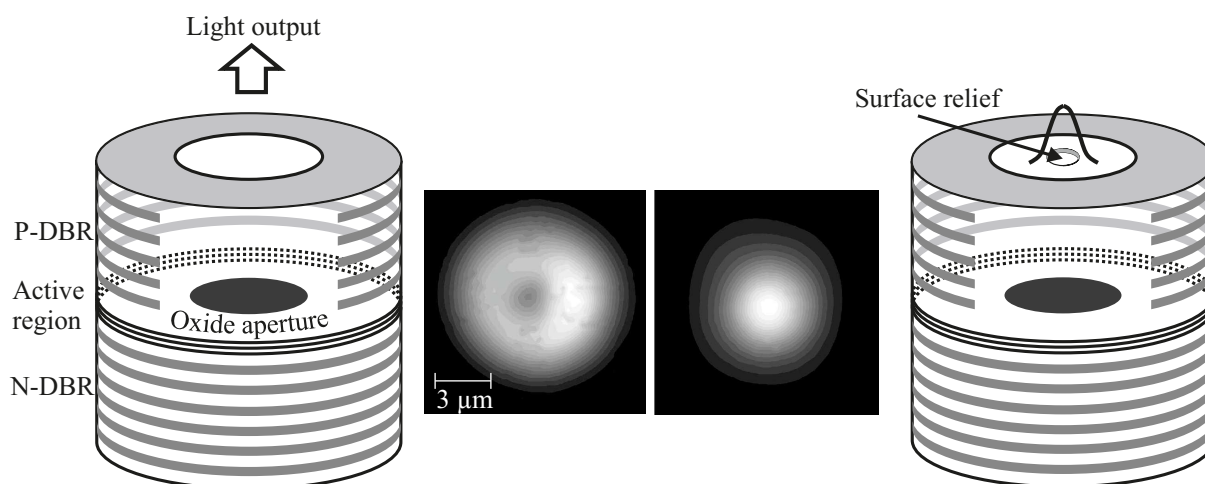


Fig. 3: Left: schematic of a standard VCSEL structure with a typical donut-like near-field intensity distribution. Right: schematic of a surface relief VCSEL with Gaussian-like intensity distribution.

An AlGaAs layer with a high aluminum content located above the active region is selectively oxidized after mesa etching, thus providing current confinement on the p-doped side. The diameter of the remaining oxide aperture strongly influences the VCSEL behavior. With a small enough diameter, for instance, a Gaussian-like beam profile can be achieved. Unfortunately, by current apertures of only up to $4\ \mu\text{m}$, the output power is limited to about 3 mW. With larger apertures it is possible to get much higher output powers. However, large active diameters result in a larger beam divergence and in the emission of higher-order transverse modes with an often donut-shaped beam profile, as shown in Fig. 3. A donut- or ring-like intensity distribution is undesirable for the intended trapping scheme because it leads to an offset between beam and trapping center [14]. Furthermore, because of the lower beam quality, the beam diameter at the focal point is increased.

The right part of Fig. 3 shows one possibility to achieve Gaussian-like emission without being limited that strongly in the optical output power. On top of the p-doped DBR, an antiphase layer with a thickness of one quarter of the material wavelength is additionally grown. By reducing the top mirror reflectivity, the antiphase layer increases the threshold gain significantly. During the VCSEL fabrication process, the antiphase layer is selectively removed in the center of the laser facet. As a result, the threshold gain is reduced only in the center to favor a Gaussian-like beam profile. The corresponding intensity distribution of a laser with a so-called surface relief is shown in the inset in Fig. 3.

Because VCSELs offer the advantageous possibility of creating various two-dimensional arrays, it is very obvious to realize patterns of optical traps, so-called optical lattices. An ultra-dense spacing of the VCSELs is highly desirable for such optical lattices and

a challenging requirement. The typical device pitch for commercial VCSELs for data communication applications is $250\ \mu\text{m}$ [15]. For interruption-free optical manipulation this value needs to be reduced by an order of magnitude. Such a drastic reduction requires not only a minimized distance between adjacent mesas of about $2\ \mu\text{m}$, but also mesa diameters reduced to around $25\ \mu\text{m}$. For an exact alignment between surface relief and active aperture, a multiple-resist self-aligned fabrication process is used, which is shown in Fig. 4.

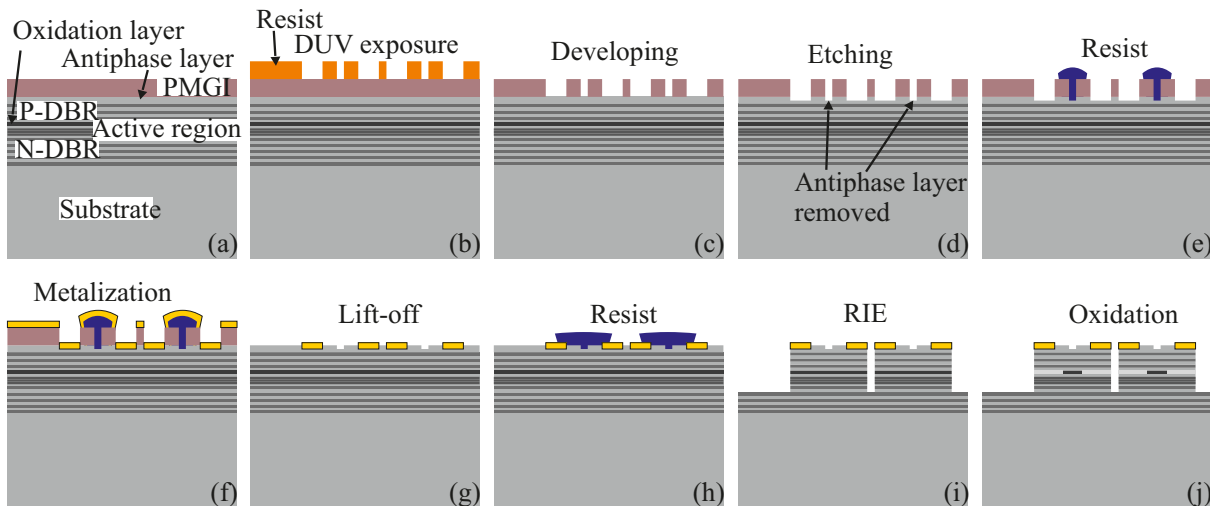


Fig. 4: Processing steps for the fabrication of densely packed VCSEL arrays. By means of a multi-layer resist self-alignment process, surface relief and oxide aperture are exactly aligned to each other. Reactive-ion etching provides for the needed vertical side walls for close spacing.

In the first step, relief and p-ring contact are defined at the same time in a PMGI (poly-methylglutarimide) resist (a). Contrary to other photoresists, PMGI requires an exposure to light in the deep-ultraviolet regime. As there is no possibility to implement a photomask in the DUV exposure setup, a structured, novolak-based resist serves as the exposure mask here (b). Due to its unique properties, the PMGI is not affected by the second resist layer. After DUV exposure and developing, the upper resist can be easily removed without damaging the PMGI underneath (c). In the second step, the surface relief is structured by wet-chemical etching (d), and the relief as well as the area surrounding the lasers are covered with another resist (e) for the subsequent metalization (f) and lift-off process (g) of the p-ring contact. For the etching of the mesas, the facets are covered with yet another novolak-based resist (h). For the desired dense packing of the lasers, wet-chemical etching of the mesas is not an option. Reactive-ion etching with carefully chosen parameters provides vertical side walls for close packing (i). As the p-ring metalization serves as etch mask, the mesa and thus the active aperture are automatically aligned exactly to p-ring and surface relief. Afterwards, the protective resist is removed and the oxidation layer is selectively oxidized by wet oxidation (j).

In a classical tweezers setup with several lenses for beam forming [16], continuous deflection of flowing particles was achieved by means of tilted linear VCSEL arrays. Continuous deflection is enabled by the following principle [17, 18]: a particle is passing the optical

lattice, created by the linear laser array. The particle is not retained but deflected at each trap if the trapping force is in the same range as the fluidic drag force. Due to the deflection at each trap, the particle follows the tilt of the array and is thus deflected orthogonal to its initial flow direction and, in our case, directed into the upper branch of the Y-junction without any mechanical or electrical intervention. The calculated x - and y -displacements for exemplary particles with diameters of $10\ \mu\text{m}$ and $15\ \mu\text{m}$ are presented in [16].

3. Drastic Miniaturization by a Novel Integration Concept

The so-called integrated optical trap represents a strongly miniaturized version of the classical tweezers setup. The bulky setup, containing several lenses for beam collimation and focusing [16], is to be replaced by one fully integrated component. For an efficient operation of the integrated optical trap, the distance between microfluidic channel and trapping lasers must be minimized to prevent strong beam expansion. The realization of electrical contacts at the p- and n-side of the laser chip turns out to be the main challenge.

An earlier approach for the integrated optical VCSEL trap is depicted in Fig. 5. It envisioned flip-chip bonding of the laser chip to the microfluidic chip using several micrometers thick indium for both mechanical and electrical connection. On the laser side, the indium bumps for soldering are placed on bondpads, simultaneously connecting several lasers. On the microfluidic side, on the lower surface of the sealing glass, the indium bumps are connected to a metal fan-out, enabling electrical contacting of the lasers.

The major disadvantage of this integration approach lies in the insufficient heat dissipation and thus an increase in the thermal resistance due to the absence of a heat sink. Figure 6 shows the output characteristics of an array of six VCSELs, comparing the behavior on wafer (left) and in the integrated module according to the earlier approach (right). Even with permanent cooling by nitrogen purging, the maximum output power was reduced by a factor of two after integration. The temperature problem could also be seen in the

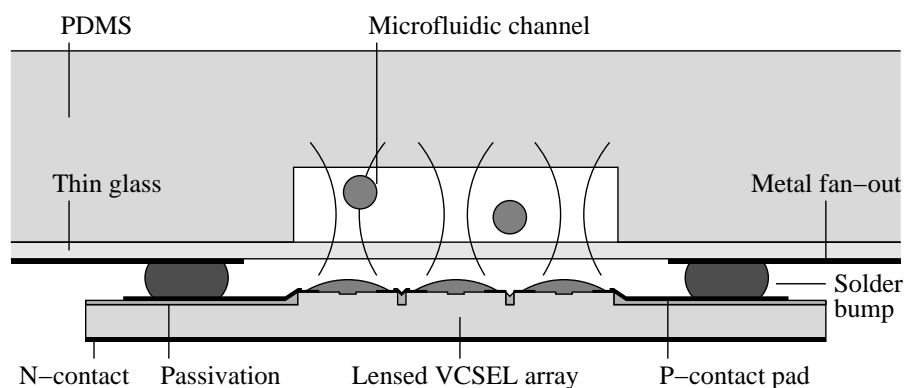


Fig. 5: Schematic of an earlier approach for the integrated optical trap array module. By indium solder bumps, the laser chip is connected both mechanically and electrically to the microfluidic chip. The VCSEL output beams are shaped by microlenses, generating weakly focused beams for particle manipulation in the microfluidic channel (from [16]).

formation and movement of bubbles in the microfluidic channel during laser operation (see inset in the right part of Fig. 6).

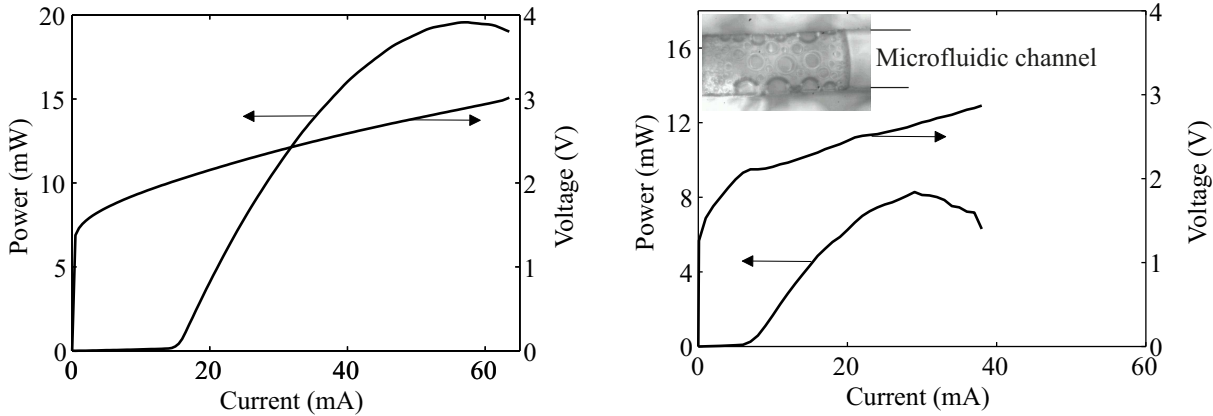


Fig. 6: Optical output power and voltage versus current of an array of six emitting VCSELs with active diameters of $6.5 \mu\text{m}$, before (left) and after (right) integration with the microfluidic chip. Due to insufficient heat dissipation, the maximum output power is reduced by a factor of two. The inset in the right graph shows the formation of bubbles in the microfluidic channel due to the elevated temperature during laser operation.

Nonetheless, we were able to show particle deflection with a device integrated according to Fig. 5. With four emitting VCSELs, we deflected a flowing particle with $15 \mu\text{m}$ diameter. Figure 7 shows snapshots of this experiment. We expect that with higher VCSEL output powers, continuous deflection would be possible at much higher flow velocities.

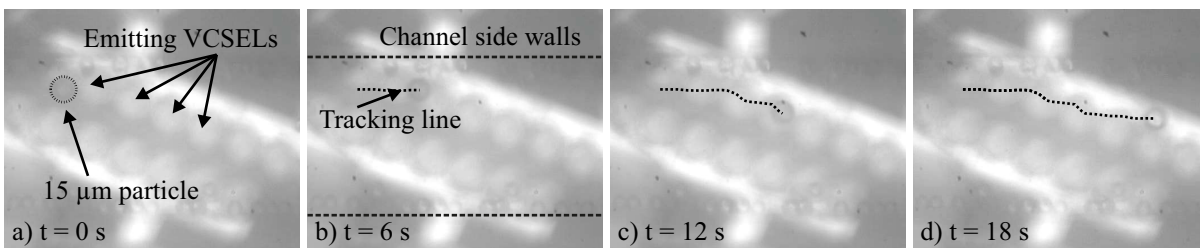


Fig. 7: Snapshots of a deflection experiment with an integrated optical trap module, realized according to the described earlier integration approach. The flowing particle is deflected by each of the emitting VCSELs (after [19]).

As mentioned above, the successful miniaturization of the VCSEL-based optical trap with avoidance of any external optics requires a minimized distance between laser facets and the microfluidic channel. However, the necessity of accessing the laser p- and n-side for electrical contacting remains. Our novel integration approach is shown in Fig. 8. It envisions to place the bondpad in a deeply etched groove in the substrate, which allows for contacting by means of bond wires. After processing, the laser chips are separated and soldered to structured heat sinks, containing several fanout tracks. The bondpads are then wire-bonded to these tracks. Microlenses on the laser facets provide slight beam shaping.

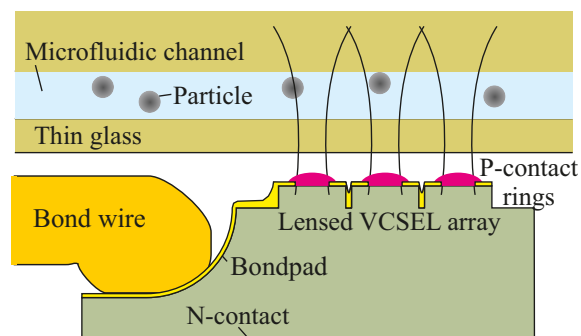


Fig. 8: Schematic of the novel integrated optical trap module. The p-contact metal is recessed, thus giving space for a thin bond wire. The back of the laser chip is accessible for n-contacting. Integrated microlenses on the laser facets achieve a weak focusing of the beams.

Earlier work [19] has shown that there is no dependence of the individual laser threshold current on the number of lasers addressed in parallel. Accordingly, we are able to connect a comparatively large number of VCSELs in parallel, in our case up to 21 per linear array. The mesa diameters range from $22\ \mu\text{m}$ to $26\ \mu\text{m}$, with active diameters between $6\ \mu\text{m}$ and $10\ \mu\text{m}$ and device pitches ranging from $24\ \mu\text{m}$ to $28\ \mu\text{m}$.

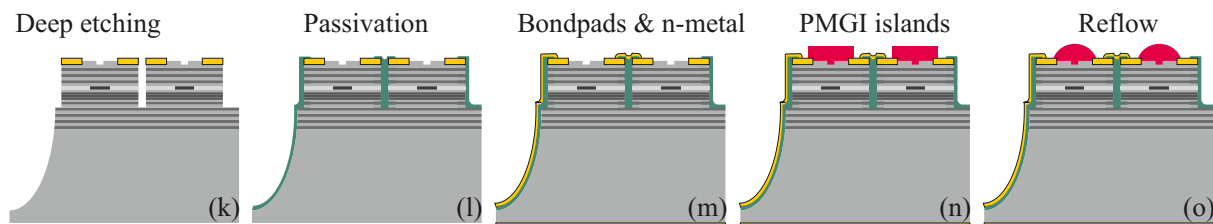


Fig. 9: Processing steps for integration-ready densely packed VCSEL arrays. After very deep etching, the side walls are passivated, then covered with metal for the bondpads. With a PMGI resist-based reflow process, microlenses are structured on the laser facets.

Figure 9 shows a schematic of the additional fabrication steps, building on the processing steps presented in Fig. 4. First, the laser arrays and the surrounding area are protected, and the bonding grooves are structured by wet-chemical etching with depths of several tens of micrometers (k). To allow the subsequent process steps, the formation of a strong undercut during groove etching has to be avoided.

As a next step, the side walls are protected with a passivation layer to prevent a short circuit between p- and n-doped layers (l). On top of the passivation, large-area bondpads are structured in the bonding grooves (m). The lithographical step for defining the bondpad metalization is difficult, especially because of the extreme topology after deep etching. During evaporation of the bondpad metalization, the samples are tilted with respect to the evaporation direction and constantly rotated. This method ensures that not only the flat surfaces but also the inclined side walls are metalized. A scanning electron microscope picture of processed VCSEL arrays with recessed bondpads is depicted in Fig. 10.

For a weak beam focusing, microlenses are structured directly on top of the laser facets. For this purpose, cylindrical islands of PMGI photoresist are structured (n), which melt

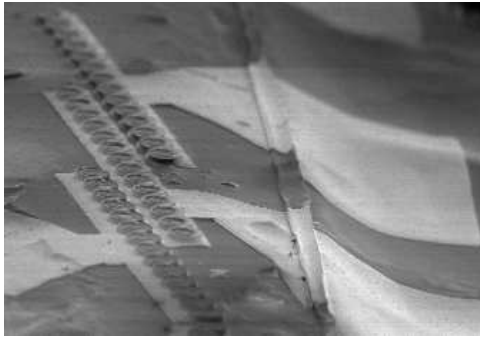


Fig. 10: Scanning electron micrograph of VCSEL arrays, fabricated according to the novel process. The bondpads can be seen in the deeply etched grooves. The length of each of the three linear 14-elements VCSEL arrays is about $390\ \mu\text{m}$.

to microlenses in the subsequent reflow process (o). With these lenses, it is possible to achieve a point of delayed divergence [19].

The output characteristics of a laser array with 16 emitting VCSELs of approximately $8\ \mu\text{m}$ active diameter is depicted in Fig. 11. Voltage and optical output power are plotted against the driving current. From the graph, a threshold current of $38\ \text{mA}$ and a maximum optical output power of $56\ \text{mW}$ can be obtained. The insets in Fig. 11 show the near-field intensity distributions of one laser in the array for three different operating currents. Dominance of the fundamental mode can be clearly seen.

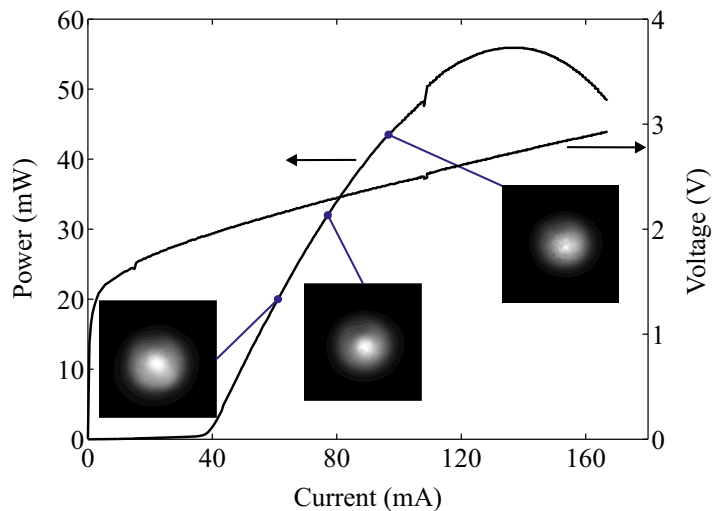


Fig. 11: Light–current–voltage characteristics of an array with 16 emitting VCSELs with $8\ \mu\text{m}$ individual active diameter. The insets show the near-field intensity distributions at three different operating currents, with a clear dominance of the fundamental mode.

4. Conclusion

In this report, we summarized the evolving progress on VCSEL arrays serving as laser sources for optical manipulation in microfluidic channels. VCSELs are excellent light sources for this purpose, thanks to their circular, high-quality beam profiles, to their low power consumption, and to their possibility of being arranged in dense two-dimensional arrays. VCSEL-based optical trapping enables compact, contamination-free particle manipulation. In classical tweezers setups, various manipulation experiments have been presented so far with solitary VCSELs or VCSEL arrays.

Our aim is the drastic miniaturization of the setup, including the development of a novel VCSEL fabrication process to achieve densely packed VCSEL arrays, with the special

feature of direct integration with the microfluidic component. The novel integration concept provides for the integration of microlenses on the laser facets for beam focusing, as well as for the possibility of electrical contacting without increased distance between lasers and microfluidics and thus loss in device performance. With the latest results, portable and inexpensive devices for VCSEL-based biological cell manipulation in microfluidics become feasible.

Acknowledgment

We thank Alexander Hein, Niazul Islam Khan, Jose Antonio Martos Calahorro, Susanne Menzel, Rudolf Rösch, Wolfgang Schwarz, and Dietmar Wahl for their support. This project was financed by the Baden-Württemberg Stiftung gGmbH.

References

- [1] A. Ashkin, “Acceleration and trapping of particles by radiation pressure”, *Phys. Rev. Lett.*, vol. 24, pp. 156–159, 1970.
- [2] A. Ashkin, J.M. Dziedzic, J.E. Bjorkholm, and S. Chu, “Observation of a single-beam gradient force optical trap for dielectric particles”, *Opt. Lett.*, vol. 11, pp. 288–290, 1986.
- [3] K. Dholakia, P. Reece, and M. Gu, “Optical manipulation”, *Chem. Soc. Rev.*, vol. 37, pp. 42–55, 2008.
- [4] D.J. Harrison, A. Manz, Z. Fan, H. Lüdi, and H.M. Widmer, “Capillary electrophoresis and sample injection systems integrated on a planar glass chip”, *Anal. Chem.*, vol. 64, no. 17, pp. 1926–1932, 1992.
- [5] J.C. McDonald and G.M. Whitesides, “Poly(dimethylsiloxane) as a material for fabricating microfluidic devices”, *Acc. Chem. Res.*, vol. 35, pp. 491–499, 2002.
- [6] N.-T. Nguyen, *Mikrofluidik*. Wiesbaden: Teubner Verlag, 2004.
- [7] R.W. Applegate Jr., J. Squier, T. Vestad, J. Oakey, D.W.M. Matt, P. Bado, M.A. Dugan, and A.A. Said, “Microfluidic sorting system based on optical waveguide integration and diode laser bar trapping”, *Lab Chip*, vol. 6, pp. 422–426, 2006.
- [8] M. Wang, M. Ozkan, E. Ata, P. Wen, M. Sanchez, C. Ozkan, O. Kibar, and S. Esener, “Integration of optoelectronic array devices for cell transport and sorting”, in *Optical Diagnostics of Living Cells*, D.L. Farkas, R.C. Leif (Eds.), Proc. SPIE 4260, pp. 68–73, 2001.
- [9] A. Kroner, J.F. May, I. Kardosh, F. Rinaldi, H. Roscher, and R. Michalzik, “Novel concepts of vertical-cavity laser-based optical traps for biomedical applications”, in *Biophotonics and New Therapy Frontiers*, R. Grzymala, O. Haeberlé (Eds.), Proc. SPIE 6191, pp. 619112-1–12, 2006.

- [10] B. Shao, S. Zlatanovic, M. Ozkan, A.L. Birkbeck, and S.C. Esener, “Manipulation of microspheres and biological cells with multiple agile VCSEL traps”, *Sensors and Actuators B*, vol. 113, pp. 866–874, 2006.
- [11] F. Sumiyama, Y. Ogura, and J. Tanida, “Fabrication of three-dimensional microscopic structure by VCSEL array trapping”, in *Optical Trapping and Optical Micromanipulation*, K. Dholakia, G.C. Spalding (Eds.), Proc. SPIE 5514, pp. 379–386, 2004.
- [12] A.L. Birkbeck, R.A. Flynn, M. Ozkan, D. Song, M. Gross, and S.C. Esener, “VCSEL arrays as micromanipulators in chip-based biosystems”, *Biomedical Microdevices*, vol. 5, pp. 47–54, 2003.
- [13] Y. Ogura, T. Beppu, F. Sumiyama, and J. Tanida, “Toward photonic DNA computing: developing optical techniques for parallel manipulation of DNA”, in *Photonics for Space Environments X*, E.W. Taylor (Ed.), Proc. SPIE 5897, pp. 34–43, 2005.
- [14] A. Kroner, I. Kardosh, F. Rinaldi, and R. Michalzik, “Towards VCSEL-based integrated optical traps for biomedical applications”, *Electron. Lett.*, vol. 42, pp. 93–94, 2006.
- [15] H. Roscher, F. Rinaldi, and R. Michalzik, “Small-pitch flip-chip-bonded VCSEL arrays enabling transmitter redundancy and monitoring in 2-D 10-Gbit/s space-parallel fiber transmission”, *IEEE J. Select. Topics Quantum Electron.*, vol. 13, pp. 1279–1289, 2007.
- [16] A. Kroner, C. Schneck, F. Rinaldi, R. Rösch, and R. Michalzik, “Application of vertical-cavity laser-based optical tweezers for particle manipulation in microfluidic channels”, in *Nanophotonics II*, D.L. Andrews, J.-M. Nunzi, A. Ostendorf (Eds.), Proc. SPIE 6988, pp. 69881R-1–12, 2008.
- [17] M.P. MacDonald, G.C. Spalding, and K. Dholakia, “Microfluidic sorting in an optical lattice”, *Nature*, vol. 426, pp. 421–424, 2003.
- [18] K. Ladavac, K. Kasza, and D.G. Grier, “Sorting mesoscopic objects with periodic potential landscapes: optical fractionation”, *Phys. Rev. E*, vol. 70, pp. 010901-1–4, 2004.
- [19] R. Michalzik, A. Kroner, A. Bergmann, and F. Rinaldi, “VCSEL-based optical trapping for microparticle manipulation”, in *Vertical-Cavity Surface-Emitting Lasers XIII*, K.D. Choquette, C. Lei (Eds.), Proc. SPIE 7229, pp. 722908-1–13, 2009.